Inorganic Materials

University of Cambridge Part III Natural Sciences Tripos

Yue Wu

Yusuf Hamied Department of Chemistry
Lensfield Road,
Cambridge, CB2 1EW

yw628@cam.ac.uk

Acknowledgements

Nothing in these lecture notes is original. They are largely based on the notes by Prof. Paul Wood, who lectured this course in 2025. Moreover, they are nowhere near accurate representations of what was actually lectured, and in particular, all errors are almost surely mine.

Preface

This course focuses on the magnetic properties of inorganic materials. It is not a theoretical course, so it will be pretty handwavy on quantum mechanical/statistical mechanical arguments. But I, as a theoretical chemist though, have tried my best to make this course notes more rigorous than the original official notes without being too pedantic.

Contents

1 Magnetism in a Single Ion

1.1 Magnetic Moment

In the 1820's Oersted showed that an electric current $\mathbf{J}$, caused by the movement of charge carriers like electrons, can generate a magnetic field given by[1]

$$\boldsymbol{\nabla} \times \mathbf{B} = \mu_0 \mathbf{J} \,, \tag{1.2}$$

where μ_0 is the permeability of free space. On the other hand, it is also found that a rotational current I in a circular wire generates something called a *magnetic moment*, $\boldsymbol{\mu}$ (or sometimes $\mathbf{m}$), given by

$$\boldsymbol{\mu} = I\hat{\mathbf{n}}A \,, \tag{1.3}$$

where A is the area enclosed by the circular wire and $\hat{\mathbf{n}}$ is the unit normal, such that placing the magnetic moment $\boldsymbol{\mu}$ in a magnetic field $\mathbf{B}$ will experience a torque

$$\boldsymbol{\tau} = \boldsymbol{\mu} \times \mathbf{B} \,. \tag{1.4}$$

This will lead to an additional potential energy

$$E = -\boldsymbol{\mu} \cdot \mathbf{B} \tag{1.5}$$

for a magnetic moment placed in a magnetic field which favours the magnetic moment to align with the magnetic field, just like an electric dipole moment will align with an electric field.
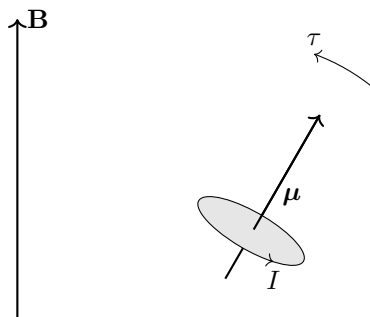

Figure 1: A charged particle with angular momentum will experience a torque in a magnetic field.

This reveals the close link between the angular momentum of a moving current and the magnetic moment. Suppose a particle of charge $+q$ of mass m is rotating around a circle of radius r with angular velocity $\boldsymbol{\omega}$. This is effectively a current

$$I = \frac{Q}{t} = \frac{\omega q}{2\pi} \,, \tag{1.6}$$

which produces a magnetic moment

$$\boldsymbol{\mu} = \frac{\boldsymbol{\omega} q r^2}{2} \,. \tag{1.7}$$

Since the particle carries an angular momentum

$$\mathbf{L} = mr^2 \boldsymbol{\omega} \,, \tag{1.8}$$

---

[1]The full form of this equation is

$$\boldsymbol{\nabla} \times \mathbf{B} = \mu_0 \left(\mathbf{J} + \epsilon_0 \frac{\partial \mathbf{E}}{\partial t} \right) \,, \tag{1.1}$$

where the latter term is something known as a *displacement current*. It comes when we're working with something like a capacitor, but we are not dealing with them in this course. Moreover, we are not distinguishing $\mathbf{H}$ and $\mathbf{B}$ and calling both of them 'magnetic field' for some reason that will be explained later.

we can conclude that the magnetic moment it creates is proportional to the angular momentum

$$\boldsymbol{\mu} = \gamma \mathbf{L} = \frac{q}{2m}\mathbf{L}\,, \tag{1.9}$$

where the proportionality constant γ is known as the *gyromagnetic ratio*. This magnetic moment, coming from orbital angular momentum (momentum caused by particle orbiting around some point), is often written with a seemingly redundant extra factor

$$\boldsymbol{\mu}_L = g_L \frac{q}{2m}\mathbf{L}\,, \tag{1.10}$$

where $g_L = 1$ is the Landé g-factor for orbital angular momentum for a reason that will be apparent immediately.

Some charge-carrying particles, like electrons, have another natural source of angular momentum — that is its spin. For a particle of spin S, it carries a spin angular momentum of magnitude

$$\|\mathbf{S}\| = \hbar\sqrt{S(S+1)}\,, \tag{1.11}$$

which also leads to a magnetic moment

$$\boldsymbol{\mu}_S = \gamma \mathbf{S} = g_S \frac{q}{2m}\mathbf{S}\,. \tag{1.12}$$

The spin of a particle does not come from its circular motion. It is intrinsic to the particle so we have no reason to assume $g_S = 1$ as for the orbital angular momentum case. For free electrons, $g_{S,e-} \approx 2.0$,[2] while for other particles like a proton, it takes some other values that are not relevant for us. For a single, isolated free electron, the magnitude of the magnetic moment is

$$\mu_S = g_S \mu_{\mathrm{B}} \sqrt{S(S+1)}\,, \tag{1.13}$$

where $S = \frac{1}{2}$, and $\mu_{\mathrm{B}} = e\hbar/2m_e$ is the Bohr's magneton (also denoted β) which characterises the strength of the magnetic moment of an electron. Note that since the charge of an electron is negative, $q = -e$, its magnetic moment $\boldsymbol{\mu}_S$ is in the opposite direction of its spin $\mathbf{S}$, i.e. the gyromagnetic ratio is negative. We will take extra care on whether we are talking about the direction of the spin or the direction of the magnetic moment in future.

1.2   Magnetic Moment of Ions and Atoms

In an ion or atom, there are two main sources of angular momenta — the spins and the orbital angular momentum of the electrons. The nucleus also carries nuclear spin, but the magnetic moment is proportional to m^{-1}, and since nuclei are much heavier than the electrons, we are ignoring the nuclear contribution.

The Schrödinger equation tells us that the electronic spins and orbital angular momentum of an atom (ion) are characterised by two quantum numbers, the total spin quantum number S and the total orbital angular momentum quantum number L. However, due to relativistic effects that are neglected in Schrödinger's equation, the spin and orbital angular momentum can interact, and the effect is that these two numbers are no longer well defined. This process is called *spin-orbit coupling*, and the overall result is that the spin is well-described by the total angular momentum quantum number J.

The strength of spin-orbit coupling is characterised by the spin-orbit coupling constant λ, and the magnitude of λ is strongly dependent on the nuclear charge, $\lambda \propto Z^4$. This means that for atoms not too heavy (up to around the third row transition metals), we can treat the spin-orbit coupling as a

---

[2]In Dirac's theory, every point-like Fermion should have $g_S = 2$ exactly, while it is actually slightly above 2 for some subtle Quantum Field Theory effects. This is known as the anomalous magnetic moment.

perturbation and still sensibly talk about the L and S values of an electronic term, and the possible J values are $J = L + S, \ldots, |L - S|$. This is the *LS coupling* (or *Russell–Saunders coupling*) scheme. For the remainder of this course, we will always assume that the spin-orbit coupling is weak enough that the LS coupling scheme always applies.

The way to work out the L, S and J values for an electronic configuration should be familiar from Part IB and Part II, and the ground term (level) is determined by the Hund's rules.

Example. Gaseous Ti^{3+} *ion.*

A free Ti^{3+} ion has electron configuration [Ar] $3d^1$. The L and S values satisfying the Hund's first and second rules can be worked out using the box method.

$$m_\ell = \quad 2 \quad 1 \quad 0 \quad -1 \quad -2$$

This gives $L = 2$ and $S = \frac{1}{2}$, with spin multiplicity $2S + 1 = 2$. The available J values are $J = \frac{5}{2}, \frac{3}{2}$. This is less than half-filled, so we need to minimise J, giving $J = \frac{3}{2}$. The ground level is therefore $^2D_{\frac{3}{2}}$.

$$\text{—— } J = \tfrac{5}{2}$$

$$\text{—— } J = \tfrac{3}{2}$$

1.2.1 Free Ions

When both the electronic spin and angular momentum are present in a free ion (atom), the overall magnetic moment is proportional to the total angular momentum:

$$\mu_J = g_J \mu_B \sqrt{J(J+1)}, \tag{1.14}$$

where the Landé g-factor for the total angular momentum is given by the complicated formula

$$g_J = g_L \frac{J(J+1) - S(S+1) + L(L+1)}{2J(J+1)} + g_S \frac{J(J+1) + S(S+1) - L(L+1)}{2J(J+1)}. \tag{1.15}$$

We have $g_L = 1$, and if we take $g_S = 2$, the above equation simplifies to

$$g_J \approx 1 + \frac{J(J+1) + S(S+1) - L(L+1)}{2J(J+1)}. \tag{1.16}$$

1.2.2 Transition Metal Complexes

Free atoms and ions are of little interest to chemists. Instead, the materials showing the most interesting magnetic properties are the transition metal complexes, which will be the main topic of this course.

The above equation cannot be directly applied to transition metal complexes, because we need a bit extra considerations on the orbital angular momentum.

We now make the claim that for an ion to carry orbital angular momentum, it must have a set of partially filled degenerate orbitals. This can be seen from the atomic orbitals: an orbital with angular

momentum quantum number ℓ is $(2\ell + 1)$-degenerate, and the non-degenerate s-orbital carries zero orbital angular momentum. The reason is that if several orbitals are degenerate, then any complex linear combination of them is also an allowed stationary state. The electron can occupy a coherent superposition with relative phases which evolve in a way such that it produces a probability density that circulates around the nucleus, leading to orbital angular momentum — this can be imagined by electrons hopping between degenerate orbitals at different orientations.

However, the degeneracies of the valence d orbitals are broken in transition metal complexes due to ligand field splitting. This leads to the quenching of the orbital angular momentum. For example, in an octahedral complex, the d orbitals are split into a T_{2g} set and a E_g set. The E_g set is only doubly degenerate, and since the orbital angular momentum quantum number can only be integers, it can carry no momentum. The T_{2g} set, on the other hand, are triply degenerate, and can carry one unit of angular momentum. Hence, if an octahedral complex has term symbol A or E, it effectively has $L_{\text{eff}} = 0$, and we say that the angular momentum is completely quenched, while a complex with term symbol T is partially quenched, and has $L_{\text{eff}} = 1$.

Example. Ground state term symbols and orbital angular momentum of octahedral complexes.

Co^{2+}, d^7 HS	Cr^{2+}, d^4 HS	Mn^{2+}, d^5 HS
T	E	A
$L_{\text{eff}} = 1$.	$L_{\text{eff}} = 0$.	$L_{\text{eff}} = 0$.
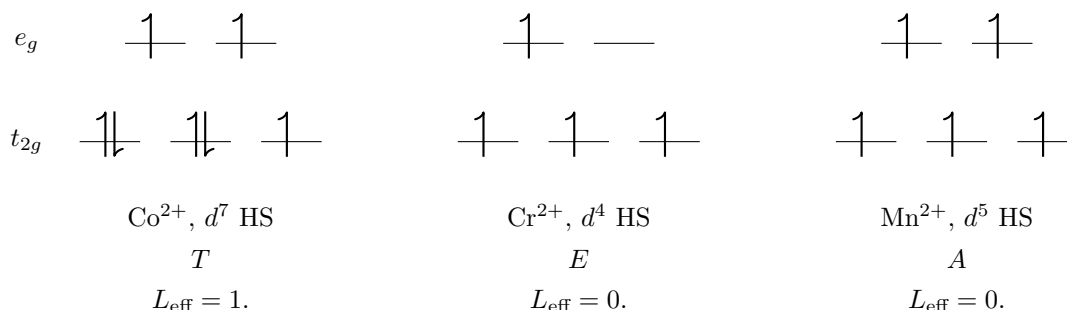
To avoid this complication, it is often good enough to only consider the contribution of the electron spins to the magnetic moment. This leads to the spin only formula

$$\mu_{\text{so}} = g_{\text{so}}\mu_{\text{B}}\sqrt{S(S + 1)} \tag{1.17}$$

for an ion of spin quantum number S. This is the formula you have seen throughout in Part IB and Part II when calculating the effective magnetic moment of e.g. a transition metal complex ion.

If we are making a very crude estimation, then we can directly take the Landé g-factor to be that of a free electron, $g_{\text{so}} \approx g_{S,e^-} \approx 2.0$. However, due to the fact that the electron is not completely free in the complexes and that we have ignored the orbital angular momentum contribution, we usually need a slightly larger value of g_{so} to match the experimental value of measured magnetic moment.

Example. Ti^{3+} *complex:* $[Ti(CN)_6]^{3-}$

Let's return to the Ti^{3+} example, but this time in a complex $[Ti(CN)_6]^{3-}$. Suppose this complex is octahedral, then the orbital diagram is shown below.
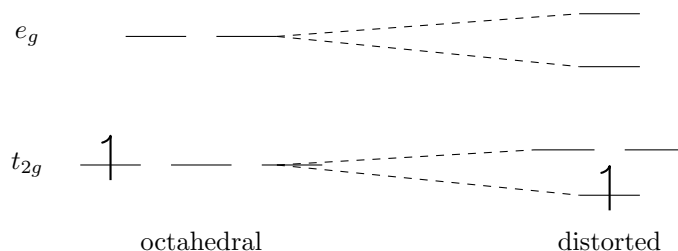
The term symbol is $^2T_{2g}$, with $L = 1$ and $S = \frac{1}{2}$. The available J values are $\frac{1}{2}$ and $\frac{3}{2}$.

However, this complex has asymmetrically filled t_{2g} level, and so it is susceptible to Jahn–Teller distortion. This further breaks the degeneracy of the t_{2g} level and leads to a complete quenching of angular momentum.

Due to the double effect of ligand field splitting and Jahn–Teller distortion, the orbital angular momentum of transition metal complexes are almost always completely quenched, and so it is fine to consider S only.

1.2.3   Lanthanide Ions

The special case comes to the lanthanide 3^+ ions. We have learned in Part II A1 that those ions have extremely contracted 4f orbitals, and the interactions between the metal ions and ligands are predominantly ionic with little covalency. As a result, the degeneracy of the 4f orbitals are not broken and they behave closely to free ions. Therefore, the formula of the magnetic moments and Landé g-factors for free ions, (1.14) and (1.16), work extremely well for lanthanide ions.

1.2.4   Spin Crossover Complex

We are familiar with the idea that a coordination complex can be classified as being either high or low spin. However, there are possibilities that the difference in crystal field stabilisation energies between the two spin states are so small that it is comparable to the thermal energy at some achievable temperature.

The most common combination of metal and ligand that gives rise to this situation is Fe (II) with moderately strong σ-donor ligands (e.g. S or N-donors). In these materials the low spin state (with $S = 0$) is always lower in energy (enthalpy) than the high spin state (with $S = 2$). However, a spin state S has degeneracy $2S + 1$, leading to an associated molar entropy

$$S_S = R\ln(2S + 1),\tag{1.18}$$

where we have assumed the orbital angular momentum to be completely quenched. For free ions or lanthanide complexes where the orbital angular momentum is significant, the corresponding entropy is

$$S_J = R\ln(2J + 1).\tag{1.19}$$

As the temperature is raised the population of the energetically excited state increases (from zero) and the sample switches from being diamagnetic to paramagnetic.

For example, consider the octahedral Fe (II) complex shown in figure 2 and the plot of μ^2 (or equivalently χT, see later) against temperature is shown in figure 3. The molecular orbital diagrams of the low spin and high spin states are shown below.

Low spin, $S = 0$
CFSE $= -\frac{12}{5}\Delta_o$

High spin, $S = 2$
CFSE $= -\frac{2}{5}\Delta_o$
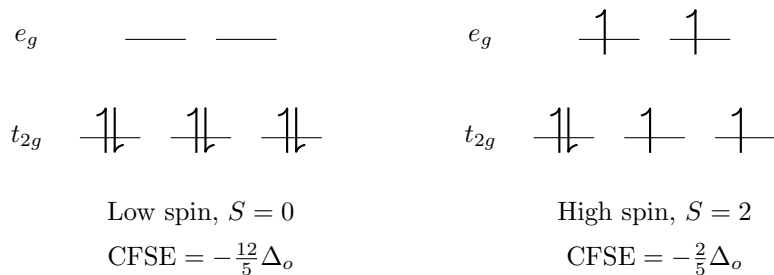
The low spin state in enthalpically favourable due to a higher |CFSE|. Assuming each pair of spin-parallel electrons contributes an exchange energy $-K$, we can estimate the enthalpy change
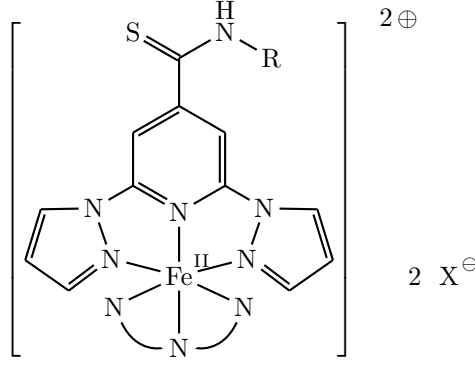
Figure 2: The structure of a spin crossover complex, where R is Me or H and X^- is BF_4^- or ClO_4^-.
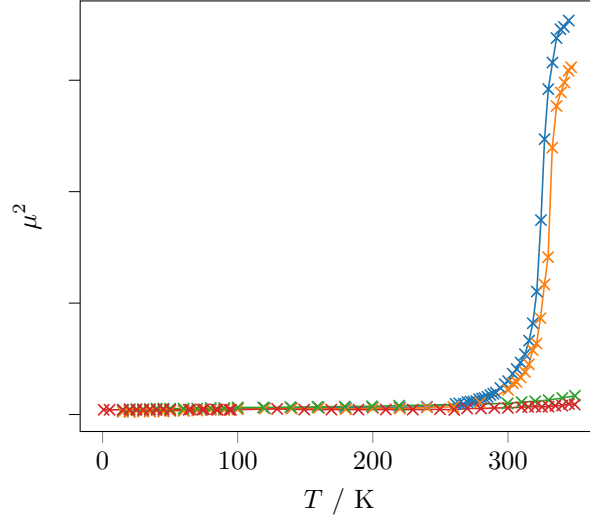

Figure 3: The μ^2 against T of a spin crossover complex. The blue and orange plots are for R = Me and the green and red points are for R = H.

from low spin to high spin to be

$$\Delta H_m \approx \left[-\frac{2}{5}\Delta_o - \binom{5}{2}K \right] - \left[-\frac{12}{5}\Delta_o - 2\binom{3}{2}K \right]$$
$$= 2\Delta_o - 4K > 0 \,, \tag{1.20}$$

where Δ_o is the octahedral crystal field splitting energy. The high spin state is entropically favoured,

$$\Delta S_m \approx R \ln S_{HS} - R \ln S_{LS} = R \ln 5 > 0 \,, \tag{1.21}$$

which allows us to estimate the spin crossover temperature

$$\Delta G_m = \Delta_r H_m - T_c \Delta S_m = 0 \quad \implies \quad T_c = \frac{\Delta H_m}{\Delta S_m} \,. \tag{1.22}$$

Note that the identity of the R group has an effect on the crossover temperature. This is because we have neglected the volumetric contribution to the enthalpy, $\Delta H_m = \Delta E_m + P \Delta V_m$. There is an associated size change when the spin state of the complex changes. Due to the different sizes of the R groups, the packing densities of the complexes in solid states might be different, and hence the ΔV_m might be different. This leads to a change in ΔH_m and hence in crossover temperature T_c.

1.3   Magnetisation in Bulk Material

The magnetic moment of a single ion is, however, difficult to measure since practically we always have a bulk material, and what we can measure is only the combined magnetic properties of the whole sample. Here, we will assume that the magnetic moments of different spin carriers are non-interacting, so the total magnetic moment of the sample, known as the *magnetisation*, is just the vector sum of all the individual magnetic moments of each ions,

$$\mathbf{M} = \sum \boldsymbol{\mu} \,. \tag{1.23}$$

We will look at this in two different perspectives — a classical perspective and a quantum perspective; the latter is apparently more correct.

1.3.1   The Classical View

Now suppose we have an ensemble of non-interacting magnetic moments that are allowed to point in any direction in space, as shown in figure 4. When there are no external magnetic fields, $\mathbf{H} = \mathbf{0}$, the magnetic moments have no preferred orientations so they are pointing in random directions. Therefore, their vector sum cancels out by symmetry and we have $\mathbf{M} = \mathbf{0}$ as shown in (a). Now suppose we are applying a small magnetic field in some direction, say $\hat{\mathbf{z}}$, $\mathbf{H} = H\hat{\mathbf{z}}$. The magnetic moments interact with the field with energy $E = -\mathbf{H} \cdot \boldsymbol{\mu}$, so they are preferred to align with the field. However, temperature will randomize the orientations of the magnetic moments since the randomized state has larger entropy than having all spins completely aligned with the field. As a result, we have a small resultant magnetisation along the applied field, $\mathbf{M} = M\hat{\mathbf{z}}$, as shown in (b). As we increase the field, there are larger preference for the spins to align with the field since the energy penalty of misalignment increases, and so the M increases, as shown in (c). This comes to a limit when all the spins are completely aligned with the field as in (d), and we reach a saturation magnetisation $\mathbf{M}_{\mathrm{sat}} = M_{\mathrm{sat}}\hat{\mathbf{z}}$.

Since in a bulk material, each magnetic moment experiences an energy $E = -\boldsymbol{\mu} \cdot \mathbf{H} = -\mu_z H$ in the magnetic field, and the magnetisation in other directions other that z cancels out so we have $M = \sum \mu_z$, we can identify that[3]

$$M = -\frac{\partial E}{\partial H} \,. \tag{1.24}$$

We further define the *magnetic susceptibility*, χ, to be the ease that the magnetisation is generated by the magnetic field,

$$\chi := \frac{\partial M}{\partial H} = -\frac{\partial^2 E}{\partial H^2} \,. \tag{1.25}$$

By the crude analysis above, we can have the rough idea that the magnetic susceptibility is large near $H = 0$, while it decreases to 0 when H is very large, since then the magnetisation will reach a saturation and further increasing H will not increase M any more.

1.3.2   The Quantum View

Now let's proceed to the quantum mechanical view of magnetisation. Now when we impose a magnetic field of strength H along $\hat{\mathbf{z}}$ direction, what it does to a quantum mechanical spin is that it creates a preferred direction, or axis of quantisation. We can therefore observe the component of spins along this direction. For a particle of spin S, its spin angular momentum along z direction spin governed by the spin magnetic quantum number, M_S, taking values $-S, -S+1, \ldots, S$. There are in total $2S+1$ of them. The spin angular momentum along this direction is $S_z = \hbar M_S$. Since the field strength is H, each of these levels have different energies

$$E = -\boldsymbol{\mu} \cdot \mathbf{H} = g\mu_{\mathrm{B}} M_S H \,. \tag{1.26}$$

---

[3]Technically, this should be Helmholtz (or Gibbs) free energy in NVT (NVP) ensembles.

(a) $H = 0$.

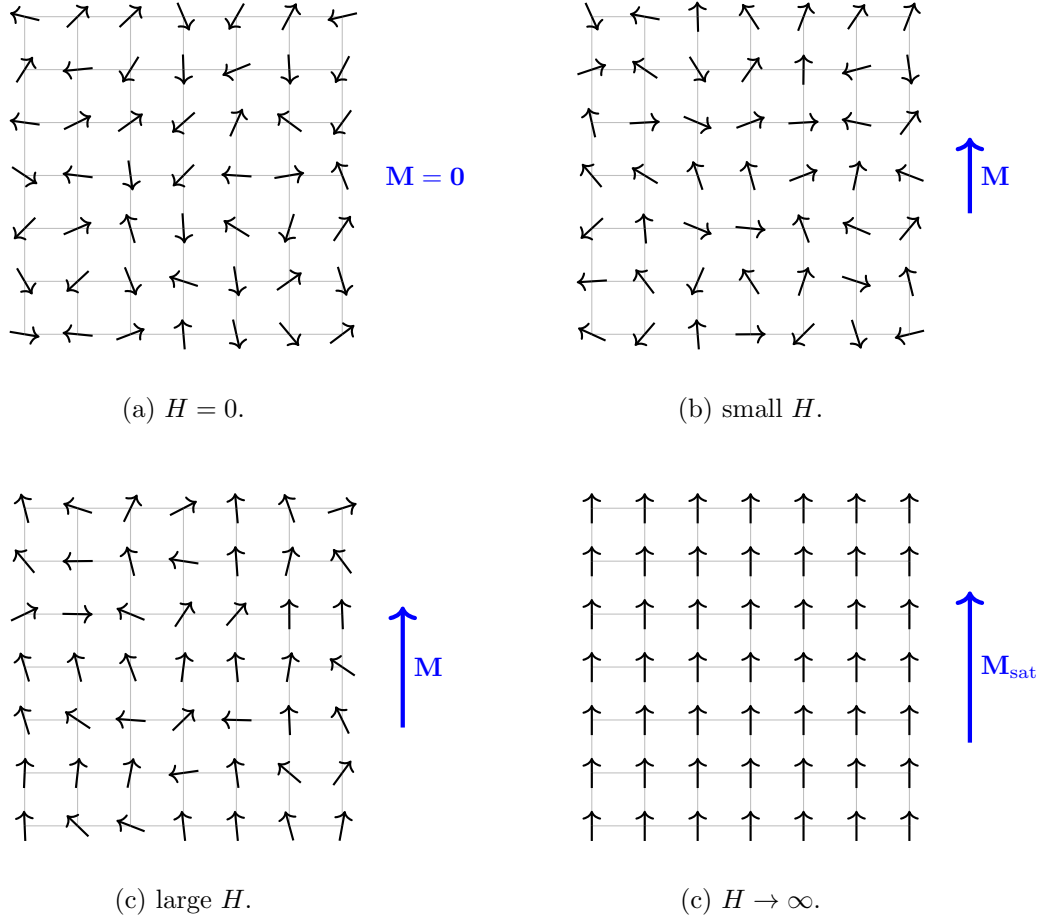(b) small H.

(c) large H.

(c) $H \to \infty$.

Figure 4: Non-interacting magnetic moments at finite temperatures with magnetic fields upward.

The negative sign disappears because recall that the gyromagnetic ratio of electron is negative so the direction of spin is opposite to that of the magnetic moment. The magnetic field breaks the degeneracies of different M_S levels, and the energy gap between levels are proportional to H.

The population of different M_S levels follows the Boltzmann distribution. When $\Delta E = g\mu_{\mathrm{B}}H \gg k_B T$, i.e. the magnetic field is large or the temperature is small, the spins will populate the lowest M_S state only. Therefore, the magnetic moments are maximally aligned with the field and we have a maximum $\mathbf{M} = \mathbf{M}_{\mathrm{sat}}$. If we decrease the field strength or increase the temperature, the thermal energy will be enough to promote the spins to higher M_S values, until when $\Delta E = g\mu_{\mathrm{B}}H \ll k_B T$, all M_S states are equally occupied, and the magnetic moments cancels so we get $\mathbf{M} = \mathbf{0}$.

1.3.3   The Brillouin Function

We can be more quantitative. The canonical thermal average of the M_S value is

$$\langle M_S \rangle = \frac{\sum_{M_S=-S}^{S} M_S e^{-\beta E(M_S)}}{\sum_{M_S=-S}^{S} e^{-\beta E(M_S)}}$$

$$= \frac{\sum_{M_S=-S}^{S} M_S e^{-\beta g\mu_{\mathrm{B}} M_S H}}{\sum_{M_S=-S}^{S} e^{-\beta g\mu_{\mathrm{B}} M_S H}}, \tag{1.27}$$
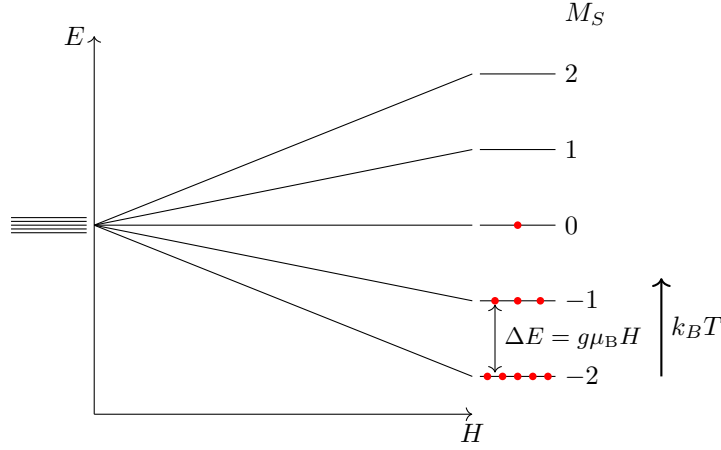
Figure 5: External magnetic field results in the splitting of the M_S levels. The occupation of the M_S levels in the canonical ensemble follows the Boltzmann distribution.

where $\beta = 1/k_B T$ is the thermodynamic inverse temperature. Denoting $\beta g \mu_B H$ as λ, this is

$$
\begin{aligned}
\langle M_S \rangle &= \frac{\sum_{M_S=-S}^{S} M_S \mathrm{e}^{-\lambda M_S}}{\sum_{M_S=-S}^{S} \mathrm{e}^{-\lambda M_S}} \\
&= \frac{-\frac{\partial}{\partial \lambda} \sum_{M_S=-S}^{S} \mathrm{e}^{-\lambda M_S}}{\sum_{M_S=-S}^{S} \mathrm{e}^{-\lambda M_S}} \\
&= -\frac{\partial}{\partial \lambda} \ln Z(\lambda) \,,
\end{aligned}
\tag{1.28}
$$

where $Z(\lambda) = \sum_{M_S} \mathrm{e}^{-\lambda M_S}$ is the partition function. This partition function is a geometric series, evaluated to

$$
Z(\lambda) = \frac{\sinh\left(\frac{(2S+1)\lambda}{2}\right)}{\sinh\left(\frac{\lambda}{2}\right)} \,,
\tag{1.29}
$$

and finally this gives

$$
\langle M_S \rangle = -\left[\frac{2S+1}{2} \coth\left(\frac{(2S+1)}{2}\lambda \right) - \frac{1}{2} \coth\left(\frac{\lambda}{2} \right) \right] \,.
\tag{1.30}
$$

It's common to define the *Brillouin function*

$$
B_S(x) = \frac{2S+1}{2S} \coth\left(\frac{(2S+1)}{2S}x \right) - \frac{1}{2} \coth\left(\frac{x}{2S} \right) \,.
\tag{1.31}
$$

This allows us to compactly write

$$
\langle M_S \rangle = -S B_S(\lambda S) = -S B_S(\beta g \mu_B S H) \,.
\tag{1.32}
$$

The molar magnetisation is therefore

$$
\begin{aligned}
M(H, T) &= -N_A g \mu_B \langle M_S \rangle = N_A g \mu_B S B_S(\beta g \mu_B S H) \\
&= N_A g \mu_B S B_S \left(\frac{g \mu_B S}{k_B} \frac{H}{T} \right) \,.
\end{aligned}
\tag{1.33}
$$

where N_A is the Avogadro's constant.

The magnetisation M is a function of $\frac{H}{T}$ only, but the functional form in pretty complex. Their plots are shown in figure 6. These plots are, however, easy to interpret. As H/T increases, the molar
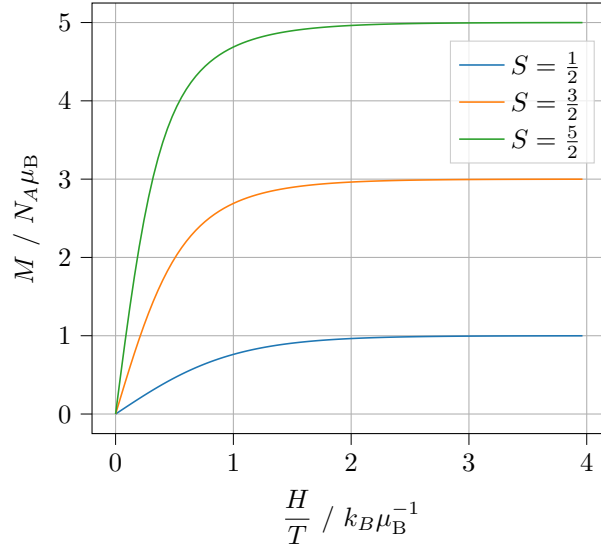
Figure 6: The magnetisation per mole of non-interacting spins against H/T, taking $g = 2$.

magnetisation monotonically increases until it reaches the saturation value $N_A g \mu_B S$, or $2S$ molar Bohr magnetons taking $g = 2$. This gives us a way of measuring the spin in bulk magnetic materials.

This high H/T limit is, however, difficult to reach since we either need a really strong magnet or a temperature close to absolute zero — both are experimentally inaccessible. We will go to this regime in experiments only if we really need to. Instead, we are more interested in the $H/T \to 0$ limit, since a small magnetic field and room temperature are trivially achievable.

1.3.4 The Curie's Law

If you look carefully, you can see that the $M(\frac{H}{T})$ graph is approximately linear in the $\frac{H}{T} \to 0$ limit, which means a constant magnetic susceptibility. The full expression of $\chi(H,T) = \frac{\partial M}{\partial H}$ needs a tough differentiation of the Brillouin function, and its full expression is meaningless to us. Instead, to look at the $\frac{H}{T} \to 0$ limit, we only need to perform a Taylor expansion in $\frac{H}{T}$. For small x, we have $\coth x \sim \frac{1}{x} + \frac{1}{3}x$, and substituting into the expression of M, we have

$$M(H,T) = \frac{N_A g^2 \mu_B^2 H S(S+1)}{3 k_B T} \, . \tag{1.34}$$

This means that for small H/T, the magnetic susceptibility is

$$\chi = \frac{M}{H} = \frac{N_A g^2 \mu_B^2 S(S+1)}{3 k_B T} \, . \tag{1.35}$$

This is independent of H (as long as H is small) and inversely proportional to T. We can write this as

$$\chi = \frac{C}{T} \, , \tag{1.36}$$

which is known as *Curie's law*, named after Pierre Curie (not Marie Curie), where

$$C = \frac{N_A g^2 \mu_B^2 S(S+1)}{3 k_B} \tag{1.37}$$

is *Curie's constant*. This law holds when

- the ground term is well isolated from any excited terms, so only the $2S + 1$ different M_S states from the same S state are populated at the temperature considered;

- there are no interactions between spins.

Note that we have $\chi T = C \propto S(S + 1)$, and we also have $\mu^2 \propto S(S + 1)$, so it is actually the macroscopic quantity χT that is actually measured in experiments, not the microscopic μ^2. Therefore, in figures like figure 3, the proper y-axis label should actually be χT, not μ^2.

A Note on Units

Whilst much of the scientific world has moved to SI units, magnetochemists have continued to work with the cgs (centimetre-gram-second) units. There is good reason to do this since it simplifies the calculations considerably.

Before we proceed, let's make clear of two easily confused quantities, the magnetic flux density (or magnetic induction) $\mathbf{B}$ and the magnetic field strength $\mathbf{H}$. What we've discussed above is the magnetic field strength $\mathbf{H}$, which measures the external magnetic field generated by free currents, not counting materials' response. However, when a external field is applied to a medium, the media respond to the external field and generates a magnetisation $\mathbf{M}$. This magnetisation also generates magnetic fields that can be experienced by other particles in the media, such as a moving charge or other magnetic moments. The total effect is the magnetic flux density

$$\mathbf{B} = \mu_0(\mathbf{H} + \mathbf{M}) \,, \tag{1.38}$$

where in SI units, the vacuum magnetic permeability $\mu_0 = 4\pi \times 10^{-7}$ N A^{-2}. The SI unit of $\mathbf{B}$ is Tesla (T = kg s^{-2} A^{-2}) and the unit of $\mathbf{H}$ is A m^{-1}. Therefore in vacuum, we have an annoying scaling between $\mathbf{B}$ and $\mathbf{H}$:

$$\mathbf{B} = \mu_0\mathbf{H} \,. \tag{1.39}$$

In the cgs unit, however, we take a different convention to move this extra 4π factor in front of $\mathbf{H}$ to somewhere in the Maxwell's equations (which doesn't affect us since we don't bother solving Maxwell's equations) so that now we have

$$\mathbf{B}_{\mathrm{cgs}} = \mathbf{H}_{\mathrm{cgs}} + 4\pi\mathbf{M}_{\mathrm{cgs}} \,, \tag{1.40}$$

and in vacuum, we have

$$\mathbf{B}_{\mathrm{cgs}} = \mathbf{H}_{\mathrm{cgs}} \tag{1.41}$$

so the magnetic field and magnetic flux density now becomes the same. The cgs unit of $\mathbf{B}$ is Gauss (G), with 1 T = $10,000$ G, and the unit of $\mathbf{H}$ is Oersted (Oe), so a magnetic field of 1 Oe produces a magnetic flux density 1 G in vacuum. The down side is that people often forget which is the correct unit of which, and tend to use them interchangeably.

Two additional units in the cgs system are the energy 1 erg = 10^{-7} J and the *electromagnetic unit* for magnetic moments 1 emu $\equiv$ 1 erg G^{-1} = 10^{-3} J T^{-1}. One mole of Bohr magnetons is $N_A\mu_{\mathrm{B}} = 5,585$ emu mol^{-1} in cgs units, and the saturation magnetisation is

$$M_{\mathrm{sat}} = gSN_A\mu_{\mathrm{B}} \approx 5,585gS \text{ emu mol}^{-1} \,. \tag{1.42}$$

The combination of constants $N_A\mu_{\mathrm{B}}^2/3k_B = 0.12504$ emu K mol^{-1} is coincidentally very close to $\frac{1}{8}$ in cgs units, which allows us to approximate the Curie's constant as

$$C = \frac{N_A\mu_{\mathrm{B}}^2}{3k_B}g^2S(S+1) \approx \frac{1}{8}g^2S(S+1) \text{ emu K mol}^{-1} \tag{1.43}$$

in cgs units. If we take $g \approx 2$, this gives us the handy formula

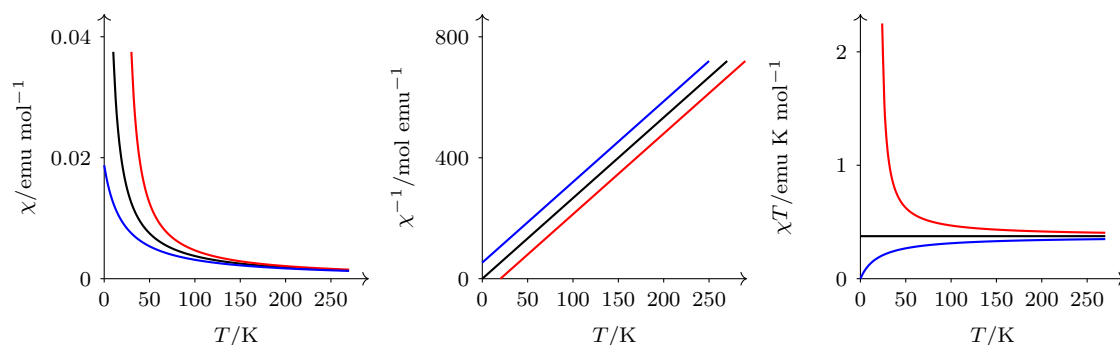$$C \approx \frac{1}{2}S(S+1) \text{ emu K mol}^{-1} \,. \tag{1.44}$$

Figure 7: Plot of χ, χ^{-1} and χT against T for spins with $S = \frac{1}{2}$, $g = 2$ and $\Theta = 0$ K (black), $\Theta = -20$ K (antiferromagnetic, blue) and $\Theta = +20$ K (ferromagnetic, red).

1.3.5   Deviation from Curie Behaviour

In many compounds, the magnetic susceptibility does not obey the Curie law, but instead obey a modified version

$$\chi = \frac{C}{T - \Theta} \tag{1.45}$$

known as the *Curie–Weiss* law for some parameter Θ known as the *Weiss constant*. This deviation from the pure Curie law can arise from a series of phenomena, including the presence of thermally accessible excited states of a single ion or some form of interaction between spin centres on neighbouring molecules. We will look at mechanisms through which they can interact later, and we will have a glimpse of how this equation arise when we introduce the Ising model. What is important is that, in both situations, there is no longer a single energy level, so our above derivation for Curie law fails.

Suppose we have two spins, quantised along some direction in the magnetic field. There are two possibilities of their relative alignments: they are either be parallel or antiparallel. If the spins are parallel, then they are said to be in *ferromagnetic alignment*, and if they are antiparallel, they are in *antiferromagnetic alignment*.

If the interaction between the two spins have an effect such that the ferromagnetic (parallel) alignment is lowered in energy than having two isolated spins and the antiferromagnetic (antiparallel) spin is raised in energy, then the two spins are said to have a *ferromagnetic interaction*. This types of interaction will encourage the alignment of spins with each other, and hence all of them tends to align with the field, leading to an increased magnetic susceptibility. This will lead to a positive Θ.

On the other hand, if the interaction between spins has an effect to encourage antiferromagnetic alignment, then this is known as an antiferromagnetic interaction, which leads to a negative Θ.

A plot of χ, χ^{-1} and χT against T are shown in figure 7. In the χ^{-1}-T graph, it is easy to read off the value of Θ by the x intercept, while in the χT-T graph, we have $\chi T \to T$ as $T \to \infty$ independent of Θ, which helps us to determine the spin S (or g value) of the molecule of interest.
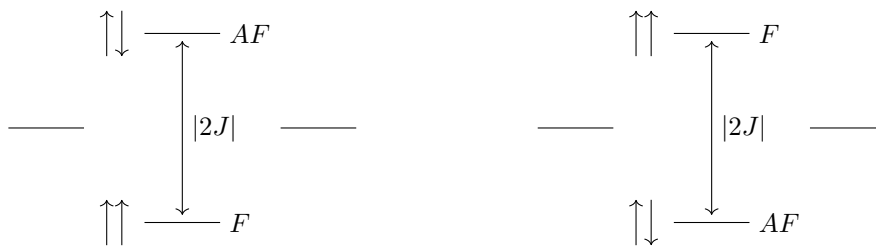
If the ferromagnetic/antiferromagnetic interactions are too strong, then the system's behaviour will deviate from the Curie–Weiss law again. In such cases, we can still fit the Curie–Weiss law to the high temperature regime, and hence we usually linearly extrapolate the high temperature data and obtain a x-intercept to determine a suitable value of Θ.

2   Magnetism in Polynuclear Species

In this section, we will examine what happens when paramagnetic ions come into close proximity and the interactions between them becomes significant.

2.1   Interactions between Two Spins

As we mentioned before, two spins have two possible alignments — ferromagnetic and antiferromagnetic alignments, and depending on the interactions between them, either of them may be lower in energy.

(i) Ferromagnetic interaction, $J > 0$.   (ii) Antiferromagnetic interaction, $J < 0$.

We define the energy difference between the antiferromagnetic alignment and the ferromagnetic alignment states to be $2J$,

$$2J = E_{\text{AF}} - E_{\text{F}}\,, \tag{2.1}$$

where J is called the *exchange parameter*. Then a ferromagnetic interaction has $J > 0$ while an antiferromagnetic interaction has $J < 0$.

We've established that the main source of magnetism in ions comes from unpaired electrons, and hence the atomic orbitals with unpaired electrons are called *magnetic orbitals*. How these magnetic orbitals interact determines whether the magnetic moments are coupled in a ferromagnetic or an antiferromagnetic way.

2.1.1   Heitler–London Model (Non-examinable)

The following discussion assumes familiarity of the contents in Part II A4: *Theoretical Techniques*.

Suppose we have two localised magnetic orbitals on two neighbouring ions, $\phi_a(\mathbf{r})$ and $\phi_b(\mathbf{r})$, each with an unpaired electron. Now we bring the two ions into proximity, so the electrons interact with the total Hamiltonian

$$\hat{H} = \hat{h}(1) + \hat{h}(2) + \frac{1}{r_{12}} \tag{2.2}$$

in atomic units, where $\hat{h}$ is the one-electron Hamiltonian. The Heitler–London model assumes the singlet (spin-antiparallel) and triplet (spin-parallel) states of the combined system to have spatial wavefunction

$$\Phi_S = \frac{\phi_a(1)\phi_b(2) + \phi_b(1)\phi_a(2)}{\sqrt{2(1 + S^2)}} \tag{2.3}$$

$$\Phi_T = \frac{\phi_a(1)\phi_b(2) - \phi_b(1)\phi_a(2)}{\sqrt{2(1 - S^2)}}\,, \tag{2.4}$$

combined with the triplet and singlet spin wavefunctions, respectively. Through some tedious algebra, the energies of the two states can be found to be

$$E_S = \left\langle \Phi_S \left| \hat{H} \right| \Phi_S \right\rangle = \frac{h_{aa} + 2Sh_{ab} + h_{bb} + J + K}{1 + S^2} \tag{2.5}$$

$$E_T = \left\langle \Phi_T \left| \hat{H} \right| \Phi_T \right\rangle = \frac{h_{aa} - 2Sh_{ab} + h_{bb} + J - K}{1 - S^2}, \tag{2.6}$$

where J is the coulomb integral and K is the exchange integral. The energy difference between the two states, expanded to order S^2, is

$$E_S - E_T \approx 2K + 4Sh_{ab}. \tag{2.7}$$

The resonance integral h_{ab} is negative, so it is common to define the *hopping integral* $t = -h_{ab}$ so that t is positive. We can recognise that the spin-antiparallel singlet state is exactly the antiferromagnetic state, and the spin-parallel triplet state is the ferromagnetic state, so we have

$$E_{\text{AF}} - E_{\text{F}} \approx 2K - 4St. \tag{2.8}$$

It is conventional to write the spin coupling Hamiltonian to be $\hat{H} = -2J\hat{\mathbf{S}}_1 \cdot \hat{\mathbf{S}}_2$, and so this energy gap is $2J$. Therefore we have

$$2J = 2K - 4St. \tag{2.9}$$

Now both $2K$ and $4St$ are positive. The $2K$ term comes from the exchange interaction between parallel spins, so when this term dominates, the system favours ferromagnetic alignment. This is sometimes known as the *potential exchange term*. The $4St$ terms arises from the electrons' ability to "hop" between atoms, which is only allowed if the electrons carry opposite spin (by Pauli exclusion principle). This leads to a reduction of the electrons' kinetic energy, and hence the system favours antiferromagnetic alignment if this term dominates. This is known as the *kinetic exchange term*.

2.2 Direct Exchange

The above formula

$$2J = 2K - 4St \tag{2.10}$$

applies when the two magnetic orbitals are close to each other so that both the exchange integral K and overlap integral S are non-negligible. This often requires the two ions to be ~ 4 Å apart or closer. This kind of interaction between unpaired spins by direct exchange interactions or electron hopping is known as *direct exchange*. Usually, unless S in negligible for some reason (e.g. $S = 0$ due to symmetry), the kinetic term tends to dominate and the coupling tends to be antiferromagnetic.

However, the metal ions in clusters are rarely close enough for these interactions to be significant, but still, communications between the spins are still clearly detected in many compounds. This suggests that there might be some indirect processes dominating the spin interactions in these species.

2.3 Superexchange

Superexchange is an indirect second order effect. It describes how two magnetic atoms that are far apart couple their spins through a non-magnetic atom, such as the ligand, that sits between them.

Inheriting the nomenclature of the direct exchange, if a superexchange favours an antiferromagnetic state, then this is known as a kinetic superexchange, while if the ferromagnetic state is favoured, it is a potential superexchange. These are best illustrated with a few examples.

2.3.1   Potential Superexchange

Potential superexchange stabilises the ferromagnetic ground state through mutually orthogonal orbitals in the exchange pathway. This is comparatively rare, but can be achieved in several ways. The most common example is a pair of 90° orthogonal orbitals in $M - L - M$, where L is a ligand.

Example. 90° $M(e_g) - O - M(e_g)$ *in* $[Cu(OH)_2Cu]^{2+}$ *dimer.*

The two metal centres in the dimer are far apart, with little orbital overlap, so direct exchange is not possible.
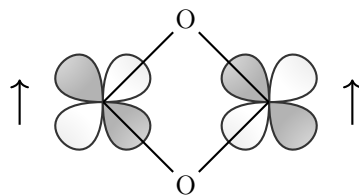
Localised orbitals (electrostatic picture)

The bonding between metal and ligand is not purely ionic (crystal field theory), but instead has a significant covalent contribution. Thus the magnetic orbital on a metal may have some ligand character. As a result, the ligand bears some spin density from both metals centres and acts as a mediator for communication between the spins formally located on metals the two centres. This brings the spin polarisations on the metals closer together and allow exchange interaction happen.
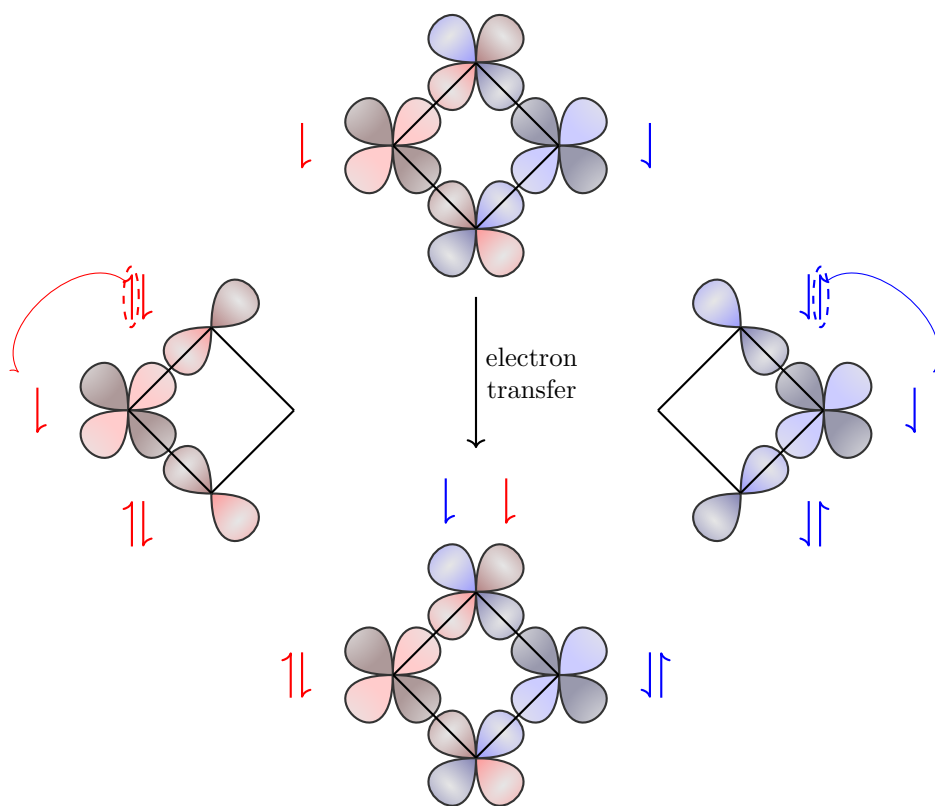
Note that the orbitals of the metals and ligands are divided into two orthogonal subsets — one labelled in red and the other in blue. A simultaneous electron hopping allows the unpaired spin density to transfer to the ligand orbitals, and now these spins are close enough to have significant exchange interaction K. Note that since the two ligand orbitals are orthogonal, the $4St$ term vanishes; this orthogonality is inherited from the orthogonality of the two metal $\mathrm{d}_{x^2-y^2}$ orbitals. Therefore, a parallel pair of spins are favoured in these ligand orbitals, which in turn favours a parallel pair of spins in the metal magnetic orbitals.

If the electrons originally in the two metal magnetic orbitals are antiparallel, then this type of electron hopping will result in an antiparallel pair of electron on oxygen, which is disfavoured by Hund's first rule. Therefore, this type of potential superexchange results in ferromagnetic interaction.

2.3.2 Kinetic Superexchange

Kinetic superexchange stabilises the antiferromagnetic ground state through overlap of two magnetic orbitals which share the same anion orbital i.e. there is a net bonding interaction between the two magnetic orbitals.

Example. $180°\ \mathrm{M}(e_g) - \mathrm{O} - \mathrm{M}(e_g)$ *interaction.*

Suppose now we have two magnetic e_g orbitals, but this time connected directly by a bridging O^{2-} at $180°$.
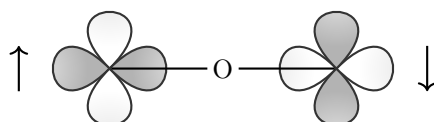
Localised orbitals (electrostatic picture)

Again ligand-metal orbital interaction covalency enables electron transfers.

electron transfer
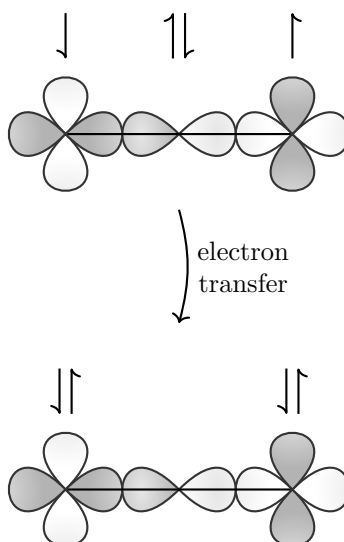
This hopping stabilisation is only possible if the two magnetic orbitals of metals initially carries opposite spins, so it results in antiferromagnetic coupling.

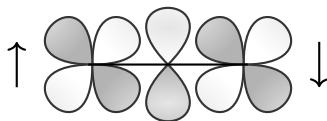The example shown above is the σ-pathway of kinetic superexchange. A π pathway is also possible between two t_{2g} magnetic orbitals, with the arrangement shown in the figure below. This is usually weaker than the σ superexchange.


2.3.3   Angular Dependence of Superexchange

As for the direct exchange, kinetic superexchange tends to dominate over potential superexchange unless S is small e.g. due to symmetry. As a result, the coupling constant J tends to have strong angular dependence.

Example. Planar copper dimers with two hydroxyl bridges.

We continue investigating the following family of planar copper dimers.
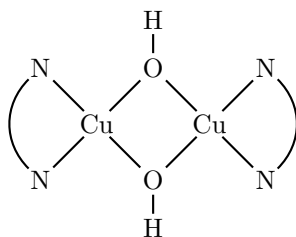
By changing the size of the $N - R - N$ ligand, we can alter the $Cu - O - Cu$ bond angle θ. When $\theta = 90°$ exactly, this is the kinetic superexchange example we met before. Since the two orbitals are orthogonal, kinetic exchange is not possible so J is positive (ferromagnetic). As the bond angle deviates from $90°$, kinetic superexchange becomes possible via scheme shown in the previous example. Hence J begins to decrease.

The J against θ is plotted in figure 8 for a range of compounds. It is found that the data shows a very good linearity against θ, with the empirical relationship

$$2J = (-74\theta + 7215) \text{ cm}^{-1} \tag{2.11}$$

for $\theta \geq 90°$ measured in degrees. Since the kinetic superexchange is much stronger than potential superexchange, we only need very small spatial overlap (via ligand) for the kinetic term to dominate — in this case $J = 0$ when $\theta = 97.5$.

From the above example, it can be seen that the ferromagnetic coupling is fragile. The potential superexchange can be easily overwhelmed by the kinetic superexchange even with only a tiny amount of spatial overlap. It seems that it is therefore very difficult to produce ferromagnetic materials like magnets — and even if we can make one by carefully controlling the geometry of orbital interaction, the small $|J|$ makes the ferromagnetic alignment easily scrambled by thermal activation once $k_B T \approx |J|$ at room temperatures.

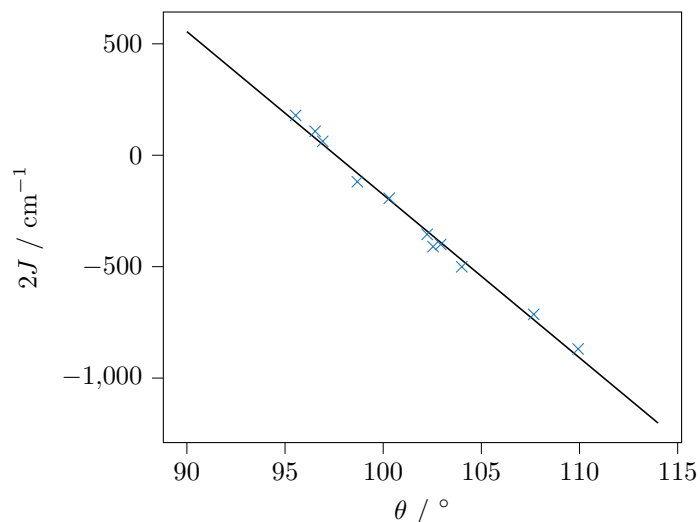We will see how this problem is resolved when we have a magnetic network.

Figure 8: The exchange parameter against ligand-metal bond angle for copper dimer.

2.3.4   General Features of Superexchange

To conclude:

- The kinetic exchange pathways are usually stronger than potential superexchange. As a consequence, when competing pathways are present the resultant interaction tends to be antiferromagnetic.

- Because of the better overlap in σ-bonds, the σ-type superexchange tends to be greater than π-superexchange, i.e. the interactions involving the e_g orbitals tend to predominate.

- The magnitude of J is very sensitive to orbital overlap (covalency). As a consequence $|J|$ tends to increase as we move from left to right (better energy match with ligand) or move down the group (more diffuse orbitals), and for softer and more polarisable ligands.

- For ions with more than one magnetic orbitals, both σ and π type interactions are possible.

2.4   Magnetic Susceptibility of Clusters

Magnetic coupling makes the susceptibility of clusters deviate from the simple Curie law — and the resulting general expression of χ is usually quite complicated: coupling splits the system to a number of energy levels, with population given by the Boltzmann distribution, and each contributes accordingly to the total magnetic susceptibility. We will first investigate the high temperature and low temperature limits, which are quite easy to work out, before discussing how to find the general expression of $\chi(T)$ for a cluster.

2.4.1   High Temperature Limit

If the temperature is high enough with $k_B T \gg |J|$, we can simply ignore the coupling and act as if the spin carriers are non-interacting. If the cluster carries spins $\{S_1, \ldots, S_n\}$, the molar susceptibility of the cluster is therefore the sum of the molar susceptibility of the individual spin carriers in the ideal Curie case,

$$\chi T = \sum_{i=1}^{n} \frac{N_A g^2 \mu_{\mathrm{B}}^2}{3k_B} S_i(S_i + 1) \,. \tag{2.12}$$

If we use $g \approx 2.0$, this gives

$$\chi T \approx \sum_{i=1}^{n} \frac{1}{2} S_i(S_i + 1) \text{ emu K mol}^{-1} \tag{2.13}$$

in cgs units.

2.4.2   Low Temperature Limit

Now, if $k_B T \ll |J|$, only the overall magnetic ground state is occupied. The whole cluster acts as like a single spin carrier with total spin S_T, so that

$$\chi T = \frac{N_A g^2 \mu_\text{B}^2}{3 k_B} S_\text{T}(S_\text{T} + 1) \approx \frac{1}{2} S_\text{T}(S_\text{T} + 1) \text{ emu K mol}^{-1} \,. \tag{2.14}$$

Note that to use Curie law, we must have $\frac{H}{T}/k_B \mu_\text{B}^{-1} \ll 1$ so that we are in the linear region of Brillouin's function. Since we take T to be small, H needs to small as well.

The total spin S_T for the magnetic ground state varies from case to case. If all the coupling within the cluster is ferromagnetic, the magnetic ground state clearly has all spins aligned so

$$S_\text{T} = \sum_{i=1}^{n} S_i \,. \tag{2.15}$$

If we have a chain of n identical spins S, then the magnetic ground state has the spins alternating in direction. If n is even, then the ground states have all spins cancelled out so $S_\text{T} = 0$, and hence

$$\chi T = 0 \,. \tag{2.16}$$

If n is odd, then we have all spins cancelled except one spin left out so $S_\text{T} = S$ and

$$\chi T = \frac{N_A g^2 \mu_\text{B}^2}{3 k_B} S(S + 1) \,. \tag{2.17}$$

If the coupling geometry is any more complex, then we need to find ground state S_T *ad hoc*.

Example. $\text{Ni}_{12}(\text{chp})_{12}(\text{OAc})_{12}(\text{H}_2\text{O})_6(\text{thf})_6$.

This complex contains twelve octahedral Ni(II) ions with $S = 1$. Using $g = 2.0$, we get the high temperature (non-interacting limit)

$$\lim_{T \to \infty} \chi T \approx 12 \times \frac{1}{2} S(S + 1) = 12 \text{ emu K mol}^{-1} \,. \tag{2.18}$$

If the metal centres are ferromagnetically coupled, then the low temperature has $S_\text{T} = 12$ and

$$\lim_{T \to 0} \chi_\text{ferro} T \approx \frac{1}{2} S_\text{T}(S_\text{T} + 1) = 78 \text{ emu K mol}^{-1} \,, \tag{2.19}$$

while if the nickel centres are antiferromagnetically coupled, the ground state has $S_\text{T} = 0$ and

$$\lim_{T \to 0} \chi_\text{anti} T \approx \frac{1}{2} S_\text{T}(S_\text{T} + 1) = 0 \text{ emu K mol}^{-1} \,. \tag{2.20}$$

We have the experimental data in figure 9. We see that the cluster's χT value increases as temperature decreases, so the coupling between Ni centres must be ferromagnetic. However, we found that the high temperature χT value levels of at around 18 emu K mol^{-1}, which is larger than our calculated value of 12 emu K mol^{-1}. This means that in this compound, we actually have a g value larger than 2.0: usually for Ni^{2+}, $g \approx 2.2$ is a good approximation, while fitting this set of data gives $g \approx 2.45$.
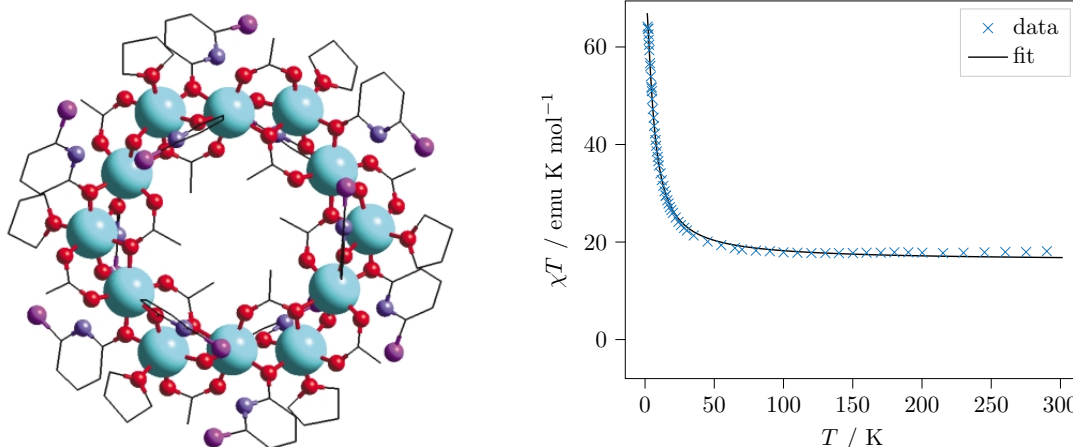
Figure 9: The structure and the measured and fitted χT against T for the Ni$_{12}$ cluster.

What we can also observe is that the χT value does not reach its low temperature limit even for the lowest-temperature data measured (1.8 K). This again suggests that the ferromagnetic coupling in this compound is really weak. Magnetic excited states with $S_T < 12$ have significant populations even at 1.8 K.

Example. $Cu_2(OAc)_4 \cdot 2H_2O$.

This cluster contains two $S = \frac{1}{2}$ Cu(II) ions. Using $g = 2.0$, the high temperature limit is

$$\lim_{T \to \infty} \chi T \approx 2 \times \frac{1}{2} S(S+1) = 0.75 \text{ emu K mol}^{-1}. \tag{2.21}$$

If the copper ions are ferromagnetically coupled, then the low temperature has $S_T = 1$ and

$$\lim_{T \to 0} \chi_{\text{ferro}} T \approx \frac{1}{2} S_T(S_T+1) = 1 \text{ emu K mol}^{-1}, \tag{2.22}$$

while if the they are antiferromagnetically coupled, the ground state has $S_T = 0$ and

$$\lim_{T \to 0} \chi_{\text{anti}} T \approx \frac{1}{2} S_T(S_T+1) = 0 \text{ emu K mol}^{-1}. \tag{2.23}$$

We have the experimental data in figure 10. It is clear to see that J is large, such that even at room temperature, χT is not approaching its high temperature limiting value. Fitting gives $J/k_B \approx 420$ K. Up until approximately 80 K, we have $\chi T \approx 0$, suggesting that only the $S_T = 0$ ground state is significantly populated at that temperature.

2.5   Modelling Exchange Interactions in Clusters

Now let's see how do we solve for the exact magnetic energy levels and $\chi T(T)$ expressions for simple systems. The recipe is as follows:

1. Set up the Hamiltonian. The *Heisenberg–Dirac–van Vleck Hamiltonian* is[4]

$$\hat{H} = -2 \sum_{i > j} J_{ij} \hat{\mathbf{S}}_i \hat{\mathbf{S}}_j, \tag{2.24}$$

---

[4]Here we assumed both the spins and the interactions are *isotropic*, i.e. the same in every direction. We will explore more possibility later.
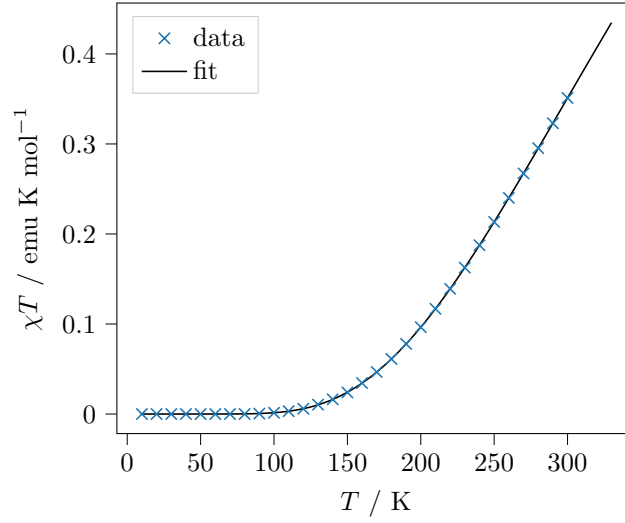
Figure 10: The measured and fitted χT against T for the Cu$_2$ cluster.

where $\hat{\mathbf{S}}_i$ is the spin operator for particle i, and J_{ij} is the coupling strength between spin i and spin j: it's positive for ferromagnetic coupling and negative for antiferromagnetic coupling.

Practically, we don't need to couple all pairs of atoms in a cluster: we only need to consider the coupling between two spin carriers if they are close enough for the interaction to be significant. This means that we can set $J_{ij} = 0$ if i and j are far enough. Moreover, some J values may be identical by symmetry, which further simplifies the expression of the Hamiltonian. A few examples of spin Hamiltonians for simple systems are given in figure 11 — we will not consider any system more complex than these in this course.

$$\hat{H} = -2J\hat{\mathbf{S}}_1 \cdot \hat{\mathbf{S}}_2$$

$$\hat{H} = -2J[\hat{\mathbf{S}}_1 \cdot \hat{\mathbf{S}}_2 + \hat{\mathbf{S}}_2 \cdot \hat{\mathbf{S}}_3 \\ + \hat{\mathbf{S}}_3 \cdot \hat{\mathbf{S}}_1]$$

$$\hat{H} = -2J[\hat{\mathbf{S}}_1 \cdot \hat{\mathbf{S}}_2 + \hat{\mathbf{S}}_1 \cdot \hat{\mathbf{S}}_3] \\ -2J'\hat{\mathbf{S}}_1 \cdot \hat{\mathbf{S}}_3$$

$$\hat{H} = -2J[\hat{\mathbf{S}}_1 \cdot \hat{\mathbf{S}}_2 + \hat{\mathbf{S}}_1 \cdot \hat{\mathbf{S}}_3 \\ \hat{\mathbf{S}}_1 \cdot \hat{\mathbf{S}}_4 + \hat{\mathbf{S}}_2 \cdot \hat{\mathbf{S}}_3 + \hat{\mathbf{S}}_2 \cdot \hat{\mathbf{S}}_4 + \hat{\mathbf{S}}_3 \cdot \hat{\mathbf{S}}_4]$$

$$\hat{H} = -2J[\hat{\mathbf{S}}_1 \cdot \hat{\mathbf{S}}_2 + \hat{\mathbf{S}}_2 \cdot \hat{\mathbf{S}}_3 \\ \hat{\mathbf{S}}_3 \cdot \hat{\mathbf{S}}_4 + \hat{\mathbf{S}}_4 \cdot \hat{\mathbf{S}}_1] - 2J'\hat{\mathbf{S}}_1 \cdot \hat{\mathbf{S}}_3$$
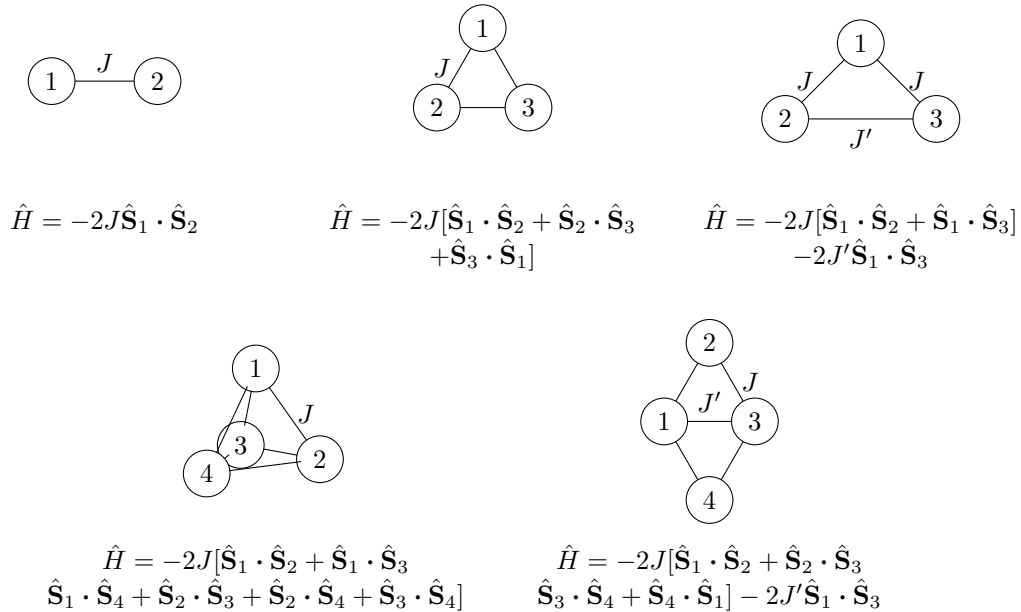
Figure 11: Examples of spin Hamiltonians of small clusters.

2. Solving the spin Hamiltonian. This is the hard bit. The brute force approach is matrix diagonalisation. This is discussed in appendix section A, assuming familiarity with quantum mechanics.

   Here we will instead use another method called *Kambe vector coupling*. It does not involve

diagonalising a matrix, and easily doable by hand for small systems. The basic idea of this method is that although we don't know the eigenvalues of $\hat{\mathbf{S}}_1 \cdot \hat{\mathbf{S}}_2$ of two spins, we do know that of $(\hat{\mathbf{S}}_1 + \hat{\mathbf{S}}_2)^2 \equiv \hat{\mathbf{S}}_{\mathrm{T}}^2$: if spin 1 has spin quantum number S_1 and spin 2 has spin quantum number S_2, then the total spin can take is quantum number S_{T} in $S_1 + S_2, S_1 + S_2 - 1, \dots |S_1 - S_2|$. Moreover, since

$$\hat{\mathbf{S}}_{\mathrm{T}}^2 = (\hat{\mathbf{S}}_1 + \hat{\mathbf{S}}_2)^2 = \hat{\mathbf{S}}_1^2 + \hat{\mathbf{S}}_2^2 + 2\hat{\mathbf{S}}_1 \cdot \hat{\mathbf{S}}_2 \,, \tag{2.25}$$

we can rewrite the coupling Hamiltonian as

$$\hat{H}_{ij} = -2J\mathbf{S}_1 \cdot \mathbf{S}_2 = J[\hat{\mathbf{S}}_1^2 + \hat{\mathbf{S}}_2^2 - \hat{\mathbf{S}}_{\mathrm{T}}^2] \,. \tag{2.26}$$

Since the eigenvalue of the squared (spin) angular momentum operator is $\hat{\mathbf{S}}^2 |S\rangle = S(S+1) |S\rangle$, the energy spectrum of $\hat{H}_{ij}$ is therefore

$$E(S_{\mathrm{T}}, S_1, S_2) = J[S_1(S_1 + 1) + S_2(S_2 + 1) - S_{\mathrm{T}}(S_{\mathrm{T}} + 1)] \,. \tag{2.27}$$

The above process solves the coupling between two spins. It can be generalised to the coupling between more spins — although it gets algebraically trickier, it is still essentially just rewriting the dot product of spin operators in terms of the squared spin operators. We will see a couple of examples later.

3. Finally, to work out the magnetic susceptibility at a certain temperature, we need to apply the Boltzmann distribution to work out the thermal average.

A state with total spin S_{T} has magnetic susceptibility

$$\chi(S_{\mathrm{T}}) = \frac{N_A g^2 \mu_{\mathrm{B}}^2}{3k_B T} S_{\mathrm{T}}(S_{\mathrm{T}} + 1) \,. \tag{2.28}$$

Suppose it has energy $E(S_{\mathrm{T}})$, since the degeneracy of the state is $2S_{\mathrm{T}} + 1$, it carries Boltzmann weight

$$(2S_{\mathrm{T}} + 1)e^{-E(S_{\mathrm{T}})/k_B T} \,. \tag{2.29}$$

The thermal (canonical) average of the magnetic susceptibility is therefore

$$\chi = \frac{N_A g^2 \mu_{\mathrm{B}}^2}{3k_B T} \frac{\sum_{S_{\mathrm{T}}} S_{\mathrm{T}}(S_{\mathrm{T}} + 1)(2S_{\mathrm{T}} + 1)e^{-E(S_{\mathrm{T}})/k_B T}}{\sum_{S_{\mathrm{T}}} (2S_{\mathrm{T}} + 1)e^{-E(S_{\mathrm{T}})/k_B T}} \,. \tag{2.30}$$

This is the *van Vleck equation*.

Let's see a couple of examples.

Example. A Cu(II)/Mn(II) *dimer.*

Let's have a look at the Cu(II)/Mn(II) complex Cu[(prp)$_2$pr]Mn(hfac)$_2$ was reported by Brewer and Sinn (*Inorg.Chem*, 1987, 26, 1529). It was studied as part of a more extended study of heteronuclear diatomics as models for the enzyme cytochrome oxidase. The structure of the Fe analogue is shown below. The two metal ions are bridged by two μ_2-phenoxy groups which are likely to provide the superexchange pathway.
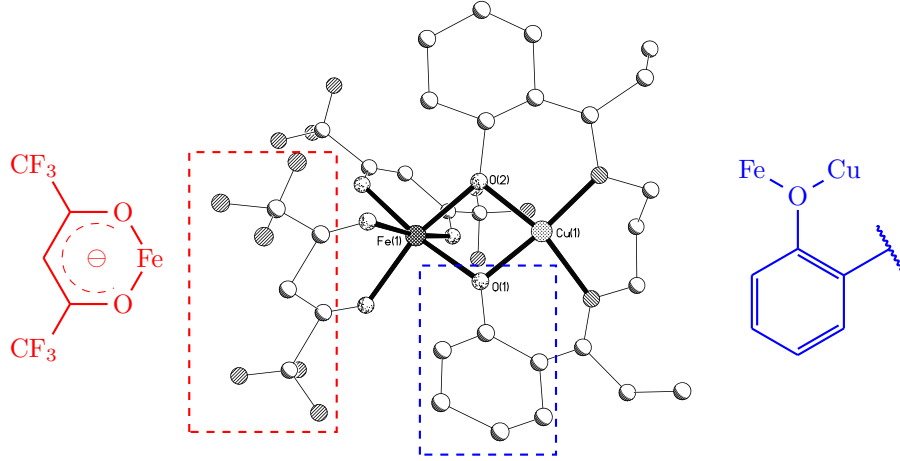
The compound has spin Hamiltonian

$$\hat{H} = -2J\hat{\mathbf{S}}_{\mathrm{Cu}} \cdot \hat{\mathbf{S}}_{\mathrm{Mn}} \,. \tag{2.31}$$

Cu$^{\mathrm{II}}$ and Mn$^{\mathrm{II}}$ have spins $S_{\mathrm{Cu}} = \frac{1}{2}$ and $S_{\mathrm{Mn}} = \frac{5}{2}$ respectively. When the two ions couple, the total spin S_{T} takes values $S_{\mathrm{T}} \in \{S_{\mathrm{Cu}} + S_{\mathrm{Mn}}, \dots, |S_{\mathrm{Cu}} - S_{\mathrm{Mn}}|\} = \{3, 2\}$.

Using the Kambe vector coupling method, the spin Hamiltonian can be rewritten as

$$\hat{H} = J[\hat{\mathbf{S}}_{\mathrm{Cu}}^2 + \hat{\mathbf{S}}_{\mathrm{Mn}}^2 - \hat{\mathbf{S}}_{\mathrm{T}}^2] \,, \tag{2.32}$$

Figure 12: X-ray structure of the Fe analogue $\text{Cu}[(\text{prp})_2\text{pr}]\text{Fe}(\text{hfac})_2$.

and so the energy spectrum are

$$E = J[S_{\text{Cu}}(S_{\text{Cu}} + 1) + S_{\text{Mn}}(S_{\text{Mn}}) - S_{\text{T}}(S_{\text{T}} + 1)]$$
$$= J\left[\frac{19}{2} - S_{\text{T}}(S_{\text{T}} + 1)\right].$$

(2.33)

The energy eigenvalues are tabulated as follows.

S_{Cu}	S_{Mn}	S_{T}	E
$\frac{1}{2}$	$\frac{5}{2}$	3	$-\frac{5}{2}J$
$\frac{1}{2}$	$\frac{5}{2}$	2	$+\frac{7}{2}J$

A convenient sanity check of the solutions obtained is that the 'centre of mass' of these energy levels, accounting for the degeneracies, should be zero:

$$\sum E(S_{\text{T}})(2S_{\text{T}} + 1) = 0.$$

(2.34)

Now, applying the van Vleck equation, we get the temperature-dependent magnetic susceptibility

$$\chi = \frac{N_A g^2 \mu_{\text{B}}^2}{3k_B T} \frac{84\text{e}^{6J/k_B T} + 30}{7\text{e}^{6J/k_B T} + 5}.$$

(2.35)

The experimental χT value of this compound is shown in figure 13. Our theoretical model fits the data really well, giving $J/k_B = -21$ K and $g = 2.05$. The coupling is antiferromagnetic.

We can also double check the high temperature and low temperature limit. When $T \to 0$, only the $S_{\text{T}} = 2$ ground state is occupied, giving

$$\lim_{T \to 0} \chi T = \frac{1}{8} g^2 S_{\text{T}}(S_{\text{T}} + 1) \approx 3.15 \text{ emu K mol}^{-1}$$

(2.36)

using the fitted g value of 2.05. (An *a priori* estimation using $g \approx 2.0$ would give $\chi T \to 3.0$ emu K mol^{-1}.) The high temperature limit is

$$\lim_{T \to \infty} \chi T = \frac{1}{8} g^2 \sum_i S_i(S_i + 1) = 4.99 \text{ emu K mol}^{-1}$$

(2.37)

using $g \approx 2.05$ ($g = 2.0$ gives $\chi T \to 3.75$ emu K mol^{-1}). We see that our graph hasn't reached this limit yet.
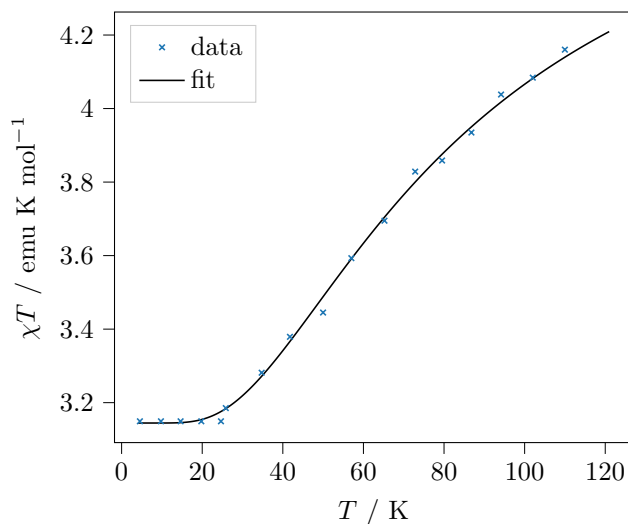
Figure 13: Experimental temperature dependence of χT for $\text{Cu}[(\text{prp})_2\text{pr}]\text{Mn}(\text{hfac})_2$.

Example. A tetrahedral tetamer $[\text{Cu}_4\text{OCl}_{10}]^{4-}$.

Reaction of $\text{CuCl}_2 \cdot 2\text{H}_2\text{O}$ with CuO and $[\text{Me}_4\text{N}]\text{Cl}$ forms an oxo-centred tetrahedral complex, $[\text{Me}_4\text{N}]_4[\text{Cu}_4\text{OCl}_{10}]$ (J.A. Bertrand and J. Kelley, *Inorg. Chem.*, 1967, 6, 495). There are two likely superexchange pathways which may contribute to the magnetic exchange; the μ_4-O and the μ_2-Cl. Magnetic data on this complex were reported by J.A. Barnes, G.W. Inman and W.E. Hatfield (*Inorg. Chem.*, 1971, 10, 1725).The temperature dependence of χT and the structure are shown in figure 14.
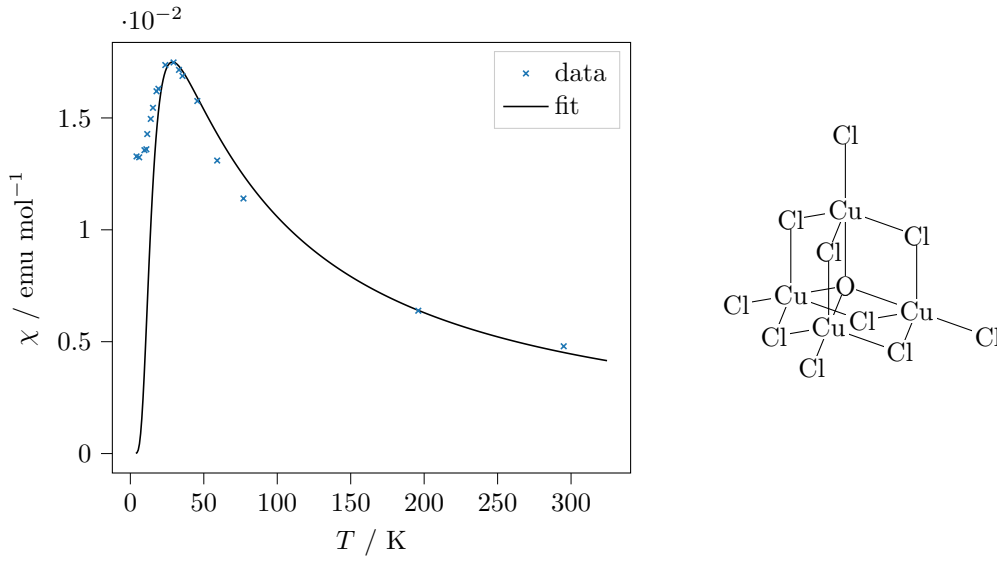
Figure 14: Structure and experimental magnetic susceptibility of $[\mathrm{Cu_4OCl_{10}}]^{4-}$.

Appendices

A   Solving Spin Hamiltonian by Matrix Diagonalisation

The most general spin interaction Hamiltonian has the form

$$\hat{H} = -2\sum_{i>j} J_{ij}^{\alpha\beta} \sum_{\alpha,\beta} \hat{S}_i^\alpha \hat{S}_j^\beta \,, \tag{A.1}$$

where the exchange parameter between two spins i and j is characterised by a 2-tensor J_{ij}. We assume that the exchange is isotropic, then this becomes

$$\begin{aligned} \hat{H} &= -2\sum_{i>j} J_{ij}\hat{\mathbf{S}}_i \cdot \hat{\mathbf{S}}_j \\ &= -2\sum_{i>j} J_{ij}[\hat{S}_i^x \hat{S}_j^x + \hat{S}_i^y \hat{S}_j^y + \hat{S}_i^z \hat{S}_j^z] \,. \end{aligned} \tag{A.2}$$

If the spin is anisotropic, e.g. if we have an Ising spin, then the transverse (x,y) components of the spin vectors are energetically suppressed. Therefore, we can ignore the x and y components in the Hamiltonian (A.2) and write

$$\hat{H} = -2\sum_{ij} J_{ij}\hat{S}_i^z \hat{S}_j^z \,. \tag{A.3}$$

This is mathematically equivalent to coupling only happening along in z directions, known as the *Ising Hamiltonian*.

We will illustrate the idea using the isotropic (Heisenberg) Hamiltonian (A.2). Our first step is to choose a basis for the N spins. A convenient choice is the direct product of the S^z basis

$$\{|S_1^z, S_2^z, \ldots, S_n^z\rangle \mid -S_i \leq S_i^z \leq S_i\} \tag{A.4}$$

with dimensionality $\prod(2S_i + 1)$. For simplicity, we will consider N spin-$\frac{1}{2}$ particles, so the basis is

$$\left\{|S_1^z, S_2^z, \ldots, S_N^z\rangle \mid S_i^z = \pm\frac{1}{2}\right\} \tag{A.5}$$

25

with dimensionality 2^N. For example, for $N = 2$, the basis set is

$$\left\{ \left| \frac{1}{2}, \frac{1}{2} \right\rangle, \left| \frac{1}{2}, -\frac{1}{2} \right\rangle, \left| -\frac{1}{2}, \frac{1}{2} \right\rangle, \left| -\frac{1}{2}, -\frac{1}{2} \right\rangle \right\}, \tag{A.6}$$

or equivalently

$$\{ |\uparrow\uparrow\rangle, |\uparrow\downarrow\rangle, |\downarrow\uparrow\rangle, |\downarrow\downarrow\rangle \}. \tag{A.7}$$

The spin operators are the representations of the $SU(2)$ group. For a spin-$\frac{1}{2}$ particle in the S^z basis, these are the *Pauli matrices*

$$\mathsf{S}^x = \frac{1}{2} \begin{pmatrix} 0 & 1 \\ 1 & 0 \end{pmatrix} \quad \mathsf{S}^y = \frac{1}{2} \begin{pmatrix} 0 & -i \\ i & 0 \end{pmatrix} \quad \mathsf{S}^z = \frac{1}{2} \begin{pmatrix} 1 & 0 \\ 0 & -1 \end{pmatrix}, \tag{A.8}$$

assuming $\hbar = 1$. In our composite space of N particles, the operator $\hat{S}_i^\alpha$ is given by the tensor product

$$\hat{S}_i^\alpha = \hat{I} \otimes \cdots \otimes \underbrace{\hat{S}^\alpha}_{\text{site } i} \otimes \ldots \hat{I}, \tag{A.9}$$

where $\hat{I}$ is the identity operator, and so

$$\hat{S}_i^\alpha \hat{S}_j^\alpha = \hat{I} \otimes \cdots \otimes \hat{S}^\alpha \otimes \cdots \otimes \hat{S}^\alpha \otimes \ldots \hat{I}, \tag{A.10}$$

with $\hat{S}^\alpha$ at sites i and j. Summing all the matrices up, we will get the full Hamiltonian in the S^z representation.

For example, for the simplest Heisenberg Hamiltonian

$$\hat{H} = -2J\hat{\mathbf{S}}_1 \cdot \hat{\mathbf{S}}_2, \tag{A.11}$$

we have

$$\mathsf{S}^x \otimes \mathsf{S}^x = \frac{1}{4} \begin{pmatrix} 0 & 0 & 0 & 1 \\ 0 & 0 & 1 & 0 \\ 0 & 1 & 0 & 0 \\ 1 & 0 & 0 & 0 \end{pmatrix} \quad \mathsf{S}^y \otimes \mathsf{S}^y = \frac{1}{4} \begin{pmatrix} 0 & 0 & 0 & -1 \\ 0 & 0 & 1 & 0 \\ 0 & 1 & 0 & 0 \\ -1 & 0 & 0 & 0 \end{pmatrix} \quad \mathsf{S}^z \otimes \mathsf{S}^z = \frac{1}{4} \begin{pmatrix} 1 & 0 & 0 & 0 \\ 0 & -1 & 0 & 0 \\ 0 & 0 & -1 & 0 \\ 0 & 0 & 0 & 1 \end{pmatrix}. \tag{A.12}$$

Summing these up, the Hamiltonian in our representation is

$$\mathsf{H} = J \begin{pmatrix} -\frac{1}{2} & 0 & 0 & 0 \\ 0 & \frac{1}{2} & -1 & 0 \\ 0 & -1 & \frac{1}{2} & 0 \\ 0 & 0 & 0 & -\frac{1}{2} \end{pmatrix}. \tag{A.13}$$

Diagonalising this matrix gives us a set of triply degenerate eigenvectors

$$\begin{pmatrix} 1 \\ 0 \\ 0 \\ 0 \end{pmatrix}, \quad \frac{1}{\sqrt{2}} \begin{pmatrix} 0 \\ 1 \\ 1 \\ 0 \end{pmatrix}, \quad \begin{pmatrix} 0 \\ 0 \\ 0 \\ 1 \end{pmatrix}, \qquad \lambda = -\frac{1}{2}J \tag{A.14}$$

and a non-degenerate eigenvector

$$\frac{1}{\sqrt{2}} \begin{pmatrix} 0 \\ 1 \\ -1 \\ 0 \end{pmatrix}, \qquad \lambda = \frac{3}{2}J. \tag{A.15}$$

These are exactly the triplet states

$$|\uparrow\uparrow\rangle, \ |\downarrow\downarrow\rangle, \ \frac{1}{\sqrt{2}}(|\uparrow\downarrow\rangle + |\downarrow\uparrow\rangle) \qquad E_{\text{triplet}} = -\frac{1}{2}J \tag{A.16}$$

and the singlet state

$$\frac{1}{\sqrt{2}}(|\uparrow\downarrow\rangle - |\downarrow\uparrow\rangle) \qquad E_{\text{triplet}} = \frac{3}{2}J\,. \tag{A.17}$$

As you can see, the dimensionality of the matrix that we have to diagonalise goes with exponentially with the system size, so it is really a computationally expensive method for large systems.